Reduction of the Neutron Induced Noise in the Compact Neutral Particle Analyzer for LHD Deuterium Plasma Experiments*)

Tetsuo OZAKI[1)], Shuji KAMIO[1)], Takeo NISHITANI[1)], Kenji SAITO[1)], Kunihiro OGAWA[1,2)], Mitsutaka ISOBE[1,2)], Masaki OSAKABE[1,2)], Makoto KOBAYASHI[1)] and the LHD Group[1)]

[1)]*National Institute for Fusion Science, 322-6 Oroshi, Toki 509-5292, Japan*

[2)]*SOKENDAI (The Graduate University for Advanced Studies), 322-6 Oroshi, Toki 509-5292, Japan*

(Received 10 January 2019 / Accepted 8 July 2019)

The compact neutral particle analyzer (CNPA) combined with the impurity pellet measurement is one of the few instruments that can directly measure the radial high energy particle distribution in the Large Helical Device (LHD). For this purpose, it is suitable to set CNPA near LHD. On the other hand, sufficient and heavy shielding against DD-neutrons, generated in deuterium experiment, is required, especially when the deuterium neutral particle beam injection heating is applied. The shield is insufficient due to the weight limitation on the stage. However, if the neutron energy is thermalized on the detector, the neutron noise can be estimated only from the total neutron yield, which is monitored by the ^{235}U fission chamber, etc. In the experiments, the pure neutron noise on the CNPA has been measured by closing the gate-valve to avoid the charge exchange neutral particle signals. The neutron noise on the CNPA has been proportional to the total neutron yield over three-order magnitudes. This means that the neutron noise can be estimated from the total neutron yield. Therefore, the calibrated charge exchange neutral signal can be obtained simply by subtracting the estimated neutron noise from the measured signal in ordinary experiments.

Keywords: CNPA, neutral particle, LHD, NBI, neutron, neutron noise, activation

DOI: 10.1585/pfr.14.3402142

1. Introduction

The Large Helical Device (LHD) [1] is a helical device with a major radius of 3.9 m and a small radius of 0.6 m with toroidal number $m = 10$, poloidal number $l = 2$. The helical type fusion reactor has an economical advantage compared with the tokamak reactor due to the ability of higher beta and steady state operation, etc. However, there are loss mechanisms of high energy particles such as loss cone, various instabilities, and charge exchange loss [2]. Therefore, the confinement of high energy particles is very important, and it is the key issue to realize the helical reactor. Several energetic particle detectors are installed in LHD [3–6]. They observe the energetic particles from the tangential and perpendicular directions, or directly observe the loss particles. The compact neutral particle analyzer (CNPA) [7] is installed in the perpendicular direction against the plasma, mainly to observe the trapped particles from the perpendicular injection beam here. CNPA observes fast neutral particles, which emit from the plasma by the charge exchange of energetic particles with background neutrals or pellets, etc. The merit of this instrument is the ability of the radial spatial distribution of high energy particles from the time history of the signal by combining with impurity pellets (PCX) [8, 9]. Therefore, it is necessary to locate CNPA just behind the impurity pellet injector (TESPEL) [10] near LHD.

The authors have measured the radial high energetic particle distribution. The heating layer, where energetic particles are rich has been identified by the PCX when the ion cyclotron range heating (ICH) is applied [11]. This measurement is also important in the deuterium plasma. Particularly, in the hydrogen minority heating with deuterium plasma of ICH, an identification of the heating region is interesting physics. In addition, we have accumulated much data in hydrogen plasmas concerning the resistive exchange mode [12], plasma wall interaction, etc. The same installation position is desirable to compare the results in hydrogen with these in deuterium.

However, CNPA has been exposed by extremely strong neutrons at the deuterium experiments started from 2017. According to the specification in Ioffe Institute, the neutron flux of $< 1 \times 10^7$ cm^2/s is recommended [13] on CNPA detector (channeltron). For this purpose, sufficient neutron shielding is necessary.

First, we design and construct the neutron shield based on acceptable neutron noise ($< 1 \times 10^7$ cm^2/s) in CNPA. After that, the neutron shield was used for plasma experiments. Since the actual CNPA system has complicated shapes due to the device itself, cables, pipes, turbo pump,

author's e-mail: ozaki@nifs.ac.jp

*) This article is based on the presentation at the 27th International Toki Conference (ITC27) & the 13th Asia Pacific Plasma Theory Conference (APPTC2018).

and vacuum gauge, etc., there are many holes in the shielding box. Therefore, an expected shielding ability could not be obtained. However, neutrons were sufficiently thermalized, and the contribution of the fast neutrons was not so large. Here, we demonstrate that it is possible to obtain a calibrated energetic neutral particle signal simply by subtracting the neutron noise if the neutron is sufficiently thermalized around the detector even in the limited shielding.

In deuterium experiments, four different types of neutron detection systems (the energy spectrum, the spatial distribution, 14 MeV neutrons, and the total yield) are prepared in LHD [14]. The total neutron flux measurement consists of the combination of two fission chambers and a ^{3}He proportional counter. In particular, the ^{235}U fission chamber is the main detector for neutron yield. Those detectors have been calibrated by using a ^{252}Cf spontaneous fission neutron source [15]. The total neutron yield has been compared with the neutron noise in CNPA.

2. Neutron Shield Design and Construction

CNPA is settled at only 3.8 m from the plasma edge. It is difficult to place shield components without limit because the central stage has a floor load limitation. In addition, we must also pay attention to interference with neighbor devices. In CNPA, the neutral particles are re-ionized on the thin foil at the entrance. After that, ions are bent by a permanent magnet and enter the channeltron detector. Therefore, fast neutrons do not directly hit the detector if suitable shield blocks are arranged. To obtain the best shielding effect under the constrained condition, the neutron shield calculation has been performed by using Monte Carlo Neutron Transport code (MCNP) [16] in a simple calculation model in the design phase. The thickness of neutron shield (boron doped polyethylene) has been chosen so that the neutron flux becomes $< 1 \times 10^{7}$ cm^{2}/s at the detector position as mentioned in section 1.

According to a calculation using the MCNP code, the neutron flux coming directly from the LHD side (front side of the shield box) is large. In addition, there are fairly homogenized neutrons due to the multi-reflection by the LHD components, the walls, and the interior in the LHD building. Considerable neutron flux remains on the side, top, and bottom, and the rear of the CNPA shielding box. Therefore, we decided upon the shielding thickness of 25 cm on the LHD side and 15 cm on the other side. Preamplifiers and a turbo pump are also covered. Total shielding weight is suppressed to be 600 kg, which is the upper limit of the allowable stage floor load. Since the inside of the shield box becomes hot, several fans are installed to remove the heat. In addition, TESPEL pipes are arranged under CNPA. Figure 1 shows the calculation results of the MCNP.

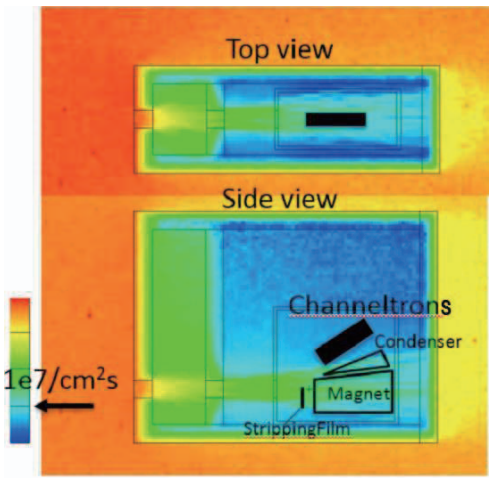

Fig. 1 Neutron distribution in CNPA by MCNP.

3. Deuterium Experiments

The most severe incident neutron comes from the inlet pipe. Half neutrons come from the inlet in the current configuration. The neutrons passing through the shield still remain. In actual experiments, sufficient shielding effect could not be achieved. There are two reasons for this. One is that MCNP calculations did not consider fine configuration in the design phase and the other is that it was difficult to manufacture the shielding box as designed.

However, according to the detailed calculation results, neutron spectra near the detector seems to be thermalized sufficiently. In order to confirm the result, indium thin foils were set in the front, rear, and inside of the shield box near the detector [17]. Two different nuclear reactions are used. One is to measure fast neutron (> 0.5 MeV) using $^{115}\mathrm{In}(n,n')\mathrm{In}^{115\,\mathrm{m}}$ reaction. Another is to measure thermal neutron (< 0.5 eV) using $^{115}\mathrm{In}(n,\gamma)\mathrm{In}^{116}$ reaction. Fast neutrons are influenced both in the front and the rear of the shield box. But fast neutrons are not observed in the inside of the shield box. From these results, the neutron seems to be almost thermalized around the detector by shielding.

In order to investigate the influence of neutron noise, the CNPA signals have been compared between the gate valve opening and closing at two similar discharges. When the gate valve is closed, the signal is obtained only from neutron. The neutron noise includes (n,γ) gamma rays although these are not a significant contribution. When the gate valve opens, the energetic neutral particles plus neutron noise are observed. We compared the signal to noise ratio (S/N) between closed and open cases in various discharge patterns as shown in Fig. 2.

S/N is very high when there is only the electron cyclotron heating (ECH) because a small amount of neutrons are generated only by thermo-nuclear reactions. In the perpendicular neutral beam injection heating (NBI) case (#4, #5), energetic neutral particles are also large amounts although the neutron amount is large because the CNPA observation position is also perpendicular. Therefore, moderate S/N can be obtained. In the tangential NBI case (#1,

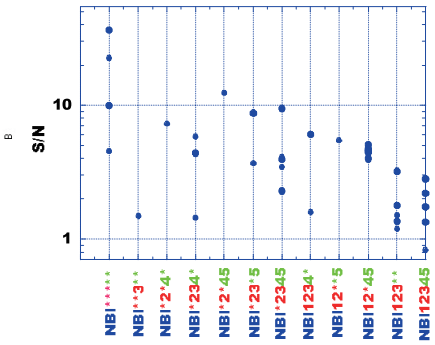

Fig. 2 Difference of S/N in various discharge patterns. NBI#1, 2, 3 and #4, 5 are injected tangentially and perpendicularly, respectively.

#2, #3), neutral particles with the tangential vector cannot be observed significantly due to the installation direction of CNPA although there are many beam-plasma neutrons. Therefore, S/N becomes extremely poor. The difference of the distance between NBI and CNPA was not sensitive. This means that we do not need to take account regarding NBI combination at the neutron noise analyzation.

The maximum observed neutron noise on CNPA is about $5 \cdot 10^6$ counts/s. Considering the efficiency of the detector and the total neutron yield, this value is not significantly different from the value predicted from the detailed MCNP calculation result.

4. Neutron Noise Estimation

In order to reduce neutron noise, increase of shielding is important. However, it is difficult to construct perfect shielding. Therefore, we tried a method to subtract the shot data at the gate valve closing from normal shot data at the gate valve opening between two similar discharges. However, it is difficult to obtain exactly the same shots even under the same conditions at all discharge patterns. According to the calculation using the MCNP code, neutrons do not directly enter, but reach the detector after the multiple scattering process, even if shielding is not enough due to holes. As a result, the thermalized neutrons are affected rather than the fast neutrons on the detector. This means that the neutron noise of the detector weakly depends on the source neutron spectrum but only on the total neutron yield.

We take account of the CNPA signal at the gate valve closing. This signal comes entirely from neutrons and relevant nuclear reactions such as (n, γ). We plot the relation (Y-C) between the neutron noise in CNPA and the total neutron yield. Since the CNPA signal is usually measured in the counting mode with time window of 0.1 ms, the signal becomes discrete. We checked the dispersion of Y-C at the different integration time. As a result, if the integration time is increased, Y-C is stabilized. But since a reasonable time-resolution as an instrument is necessary, we adopt 10 ms as the integration time. This value is the standard time step of high energy particle spectra in CNPA.

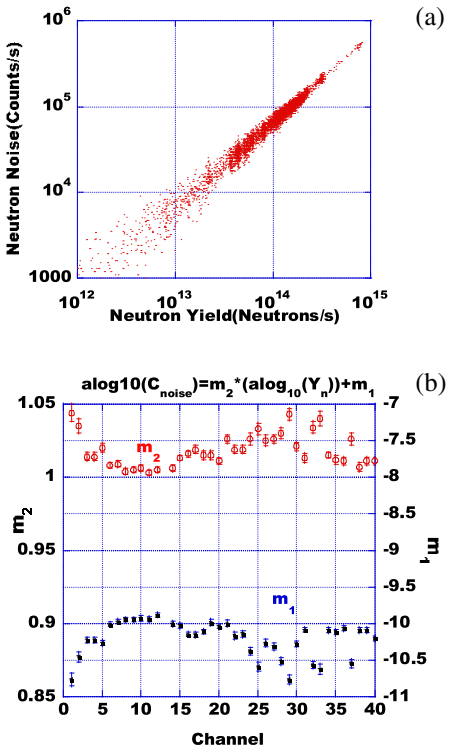

Fig. 3 Neutron noise versus neutron yield. (a) Neutron noise versus neutron yield (Y-C), (b) The factors in all channeltrons.

In Fig. 3 (a), the Y-C at a typical channeltron in CNPA is plotted. Logarithmic scales are used in both the vertical and the horizontal axes in Fig. 3 (a). Although the spectra of the neutron are different in various discharges, the neutron noise in CNPA is proportional to the neutron yield over three orders of magnitude. Therefore, if only the total neutron yield is monitored, the neutron noise in CNPA can be predicted.

Each dependence of 40 channels in CNPA between neutron yield and the neutron noise can be obtained as follows:

$$\log_{10}(C_{\mathrm{noise}}) = m_2 \log_{10}(Y_{\mathrm{n}}) + m_1, \tag{1}$$

where m_1, m_2, Y_{n}, and C_{noise} are the fitting parameters, the total neutron yield per second and the neutron noise per second, respectively. m_1 and m_2 depend on each preamplifier threshold and each channeltron character (Fig. 3 (b)). The errors of m_1 and m_2 are within $\pm 0.5\%$. The neutron noise can be estimated based on this result. The calibrated signal can be easily obtained by subtracting the neutron noise from the observed signal.

5. Obtaining Calibrated Signal

To confirm the validity of this technique, we checked whether the calibrated signal becomes zero, when the gate valve is closed. Figure 4 shows a typical example of channeltron signal at an ECH plasma discharge sustained by four NBI#2, #3, #4, and #5. When the gate valve is closed, the calibrated signal has been almost zero as shown in

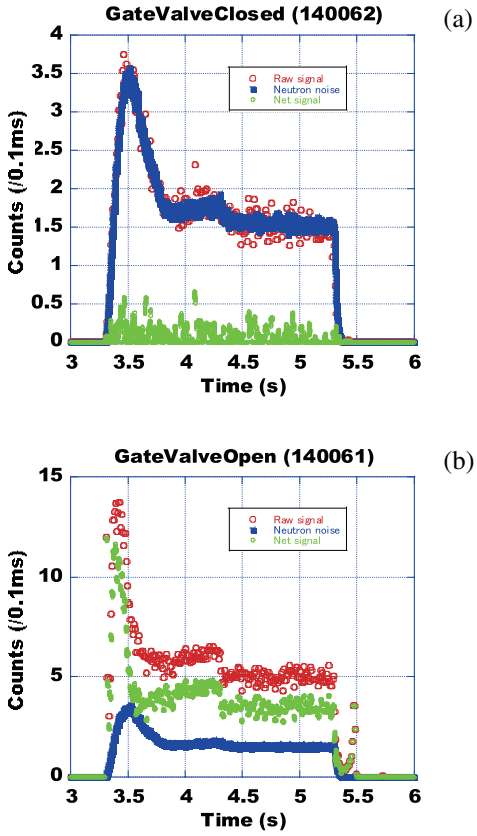

Fig. 4 Neutron noise reduction. (a) Validity check at gate valve closing, (b) Calibrated signal.

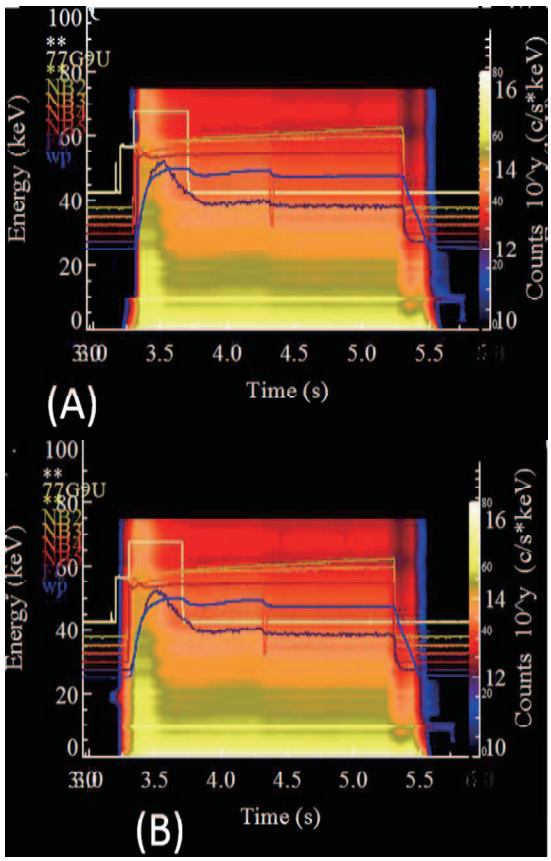

Fig. 5 Comparison between (A) and (B). (A) Net neutrons predicted by Eq. (1), (B) Subtraction between similar discharges.

Fig. 4 (a). The validity of this technique has been proved.

Calibrated energetic neutral particle signals are obtained by two methods as follows:

(A) Subtract the neutron noise predicted by Eq. (1) from the normal shot result, and

(B) Subtract the reference shot result in the gate valve closing from the normal shot result at two similar discharges.

Figure 4 (b) shows the calibrated signal obtained by (A) when the gate valve opens. To confirm the validity of (A), we compare (A) with (B) between two similar plasma discharges. Time histories of the spectra indicated by the contour plots are shown in Figs. 5 (a) and (b). The main waveforms, such as ECH (77G9U), NBIs, plasma stored energy (wp), and total neutron yield (FC) during discharge are also shown in Figs. 5 (a) and (b). Since both time histories of the spectra are in agreement completely with each other, we can establish a method to obtain calibrated energetic neutral particle signals using the total neutron yield even at the high neutron environment.

6. Summary

Neutron noise reduction is important for CNPA measurement in deuterium experiments. However, neutron shielding is not perfect due to various reasons. The neutrons are sufficiently thermalized at the detector position. The neutron noise is proportional to the total neutron yield over three orders of magnitude. Therefore, neutron noise can be predicted from the total neutron yield. By subtracting it from observation data, energetic particle spectra can be easily obtained. Plenty noise neutrons come from the beam inlet. To improve S/N ratio, oblique incident neutrons can be reduced by shielding the inlet pipe.

Acknowledgments

Authors thank NIFS for financial support from code: NIFS ULRR006.

[1] O. Motojima *et al.*, Fusion Eng. Des. **20**, 3 (1993).
[2] H. Sanuki *et al.*, Phys. Fluids **B2**, 2155 (1990).
[3] M. Isobe *et al.*, Rev. Sci. Instrum. **72**, 611 (2001).
[4] M. Osakabe *et al.*, Rev. Sci. Instrum. **75**, 3601 (2004).
[5] M. Sasao *et al.*, J. Nucl. Mater. **313-316**, 1010 (2003).
[6] T. Ozaki *et al.*, Rev. Sci. Instrum. **83**, 10D920 (2012).
[7] P. Goncharov *et al.*, Rev. Sci. Instrum. **79**, 10F312 (2008).
[8] P. Goncharov *et al.*, Rev. Sci. Instrum. **74**, 1869 (2003).
[9] T. Ozaki *et al.*, J. Plasma Fusion Res. **8**, 1089 (2009) .
[10] S. Sudo *et al.*, Rev. Sci. Instrum. **83**, 023503 (2012).
[11] T. Ozaki *et al.*, Plasma Fusion Res. **7**, 2402138 (2012).
[12] X.D. Du *et al.*, Phys. Rev. Lett. **114**, 155003 (2015).
[13] http://www.ioffe.ru/ACPL/npd/npa05.htm
[14] M. Isobe *et al.*, Rev. Sci. Instrum. **85**, 11E114 (2014).
[15] T. Nishitani *et al.*, Fusion Eng. Des. **136**, 210 (2018).
[16] T. Nishitani *et al.*, Fusion Eng. Des. **123**, 1020 (2017).
[17] M. Kobayashi *et al.*, Fusion Eng. Des. **137**, 191 (2018).